Computational Modeling and Simulation of Microfluidic Biochips for Parallel Biomolecular Synthesis

Heng-Chuan Kan

National Center for High-Performance Computing
No. 21, Nan-ke 3rd Rd., Hsinshi, Tainan County 74147, Taiwan, R.O.C.
n00hck00@nchc.org.tw

ABSTRACT

In this study, a novel microfluidics based biochip has been developed by the aid of analytical modeling and numerical simulation efforts for the purpose of massively parallel oligonucleotude-DNA (oDNA) syntheses. The microfluidic biochip consists of thousands of reaction sites interconnected by micro-channels and can be used as micro-reactors for various biochemical processes simultaneously. The impacts and implications of the efficiencies of each oDNA synthesis step during repeated synthesis cycles have been evaluated to improve the synthesis yield of final full-length products. The results from analytical model indicate the deprotection step during the oDNA synthesis cycle is a vital process for ensuring the high yield of full-length products. Numerical simulation results further reveal that the confinement of various chemical reagents within each reaction site can be well-controlled to minimize cross contamination from the neighboring reaction sites by the design of current microfluidic biochip.

Keyword: Microfluidics, DNA synthesis, Biochips

1. INTRODUCTION

Recent advances in miniaturization technology have generated significant impacts in world of chemistry, medicine, and life sciences. Accompanying by the rapid advances in research fields of Micro-Electro-Mechanical-Systems (MEMS) and Microfluidics technology have created enormous interests in various biotechnology applications in the past few decades. Contrast to traditional desktop laboratory equipments, these Microsystems offer many advantages including compact size, disposability, increased speed, parallel analyses, functionality, and decreased sample/reagent consumptions. Microfluidic systems have been shown to various applications including bio-molecular separation and detection [1-2], biological cell manipulation [3-4], and DNA amplification by Polymerase Chain Reaction (PCR) [5]. Such a system needs to be simple to fabricate, robust to operate, and preferably easy to be interfaced with detection/analysis and fluidic handling macro devices. However, the fact of lacking simple and universal parallel micro-reactors has prompted this study. It is highly desirable to be able to carry out chemical reactions involving harsh chemicals as well mild biochemical reactions in the same system.

We previously presented a liquid phase chemistry approach using photogenerated reagent that allows various otherwise non-photochemical reactions to be controlled by light [6]. Here we demonstrate the analytical modeling and numerical simulation efforts for evaluating the effects of efficiencies of each DNA synthesis step on the synthesis yield of final full-length products by a passive microfluidic biochip which consists of thousands of reaction sites carrying out highly multiplexed chemical reactions each being individually addressable with light.

2. PROBLEM DESCRIPTION

The basic function of the current microfluidic chip is to provide a desirable flow distribution and a desired chemical confinement. A critical element in the success of the proposed platform is the microfluidic array-reactor chip as shown in Figure 1(a). A working concept chip, that we have already fabricated and tested for biochip array assay applications, is shown in Figure 1(b). This concept chip is designed to include more than 8,000 different bio-molecules, measured about 20 mm x 15 mm x 1 mm, and has a total internal volume of only 10 μl. Each chip is made of a silicon substrate on which fluidic channels and reaction cells are fabricate using standard semiconductor etching processes [7]. The operation principle of the chip is as following. As shown in Figure 1a, during each synthesis step, a reagent stream flows into the array chip through an inlet channel and splits into side streams. Each reaction site can be isolated by the side walls in between. After passing through the reaction sites, the side streams merge into the draining channel and flow out of the array chip. During the deprotection step (e.g., a photochemical reaction), a fluid containing a photogenerated reagent precursor is sent into the array chip and a light beam is directed at the reaction site on the right so reagent is present inside the un-illuminated reaction on the left. Under normal flow conditions, the flow rate into the reaction site on the right is high enough to prevent the active reagent from the diffusing back into the inlet channel and thus no active reagent would enter the reaction site on the left. With this operational and structural design each individual reaction cell is dynamically isolated and a plurality of discrete chemical reactions can be conducted in parallel among any arbitrarily selected group of reaction sites.

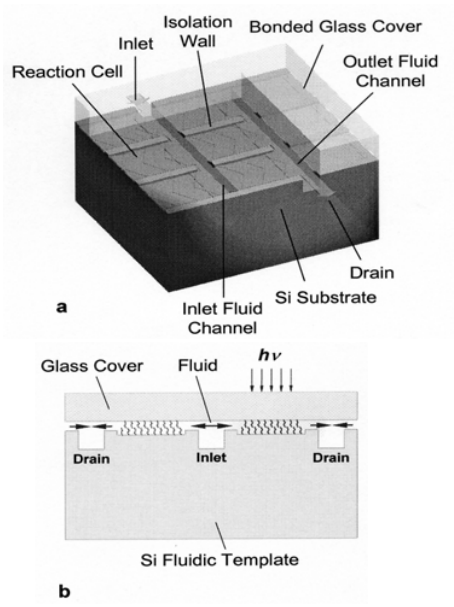

Figure 1. Schematic illustration of the structure and operation of a microfluidic array reaction chip.

3. RESULTS AND DISCUSSIONS

3.1 DNA Synthesis Model

Traditional DNA synthesis involves four major steps, namely, deprotection, coupling, oxidation, and capping during a single synthesis cycle. An analytical model which is essentially based on Stoichiometric calculations of each product was developed to assess the efficiencies of various steps. In order to achieve the high yield for synthesized long DNA sequence, the efficiency of each step has to be evaluated to better understand its limits and impacts during each synthesis cycle. Since the oxidation step does not impact the synthesis yield, only the other three efficiencies are considered here. The reference case we established here is that the efficiencies of deprotection, coupling, and capping are all equal to 99.5%. Another important parameter in the current analytical model is the probe length which is set to be a constant of 50 for all the cases. We are interested in predicting the synthesis yield of final full-length products, i.e., 50-mer. The results shown in Figure 3.1.1(a) reveal that the final synthesis yield for full-length products is about 60.6% and the rest of synthesized products is concentrated on long but non-full-length products such as 49-mer (15.84%) and 48-mer (1.9%). Figure 3.1.1(b) demonstrates the effects of deprotection efficiency on the final full length products. When the deprecation efficiency decreases from 99.5% to 98.0%, the yield of full-length products reduces from 60.6% to 28.4%. The significant drop in synthesis yield illustrates the importance of strictly controlling of PGA precursor delivery and confinement during deprotection step to avoid cross contamination from neighboring reaction cells. Note that the final synthesis yield for 49-mer is higher than that of the full-length product.

The effects of coupling efficiency are shown in Figure 3.1.2(b). The final synthesis yield of full-length products decreases from 60.6% to 28.3% as the coupling efficiency drops from 99.5% to 98.0%. However, the junk products are concentrated in much shorter length products. It is clearly seen from Figure 3.1.3 (b) that the capping step has minimal influence on the synthesis yield of final full-length products. The synthesis yield changes only slightly from 60.58% t0 60.57% when the capping efficiency drops from 99.5% to 98.0%.

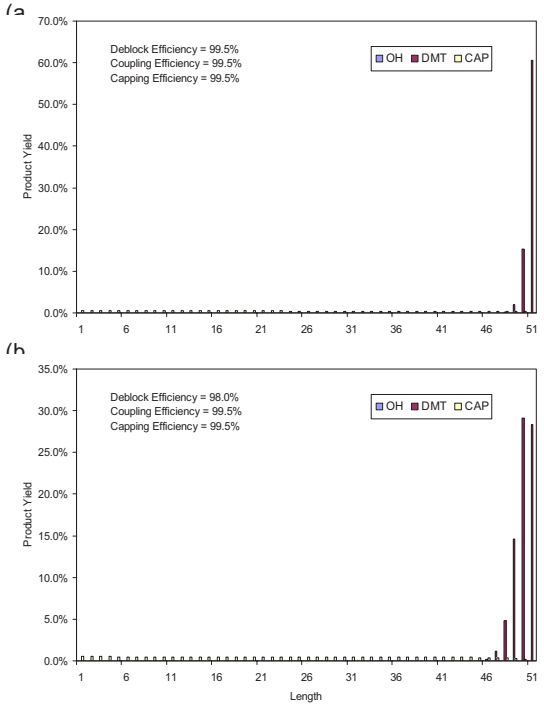

Figure 3.1.1. Effects of deprotection efficiency on the synthesis yield of final full-length products after 50 synthesis cycles.

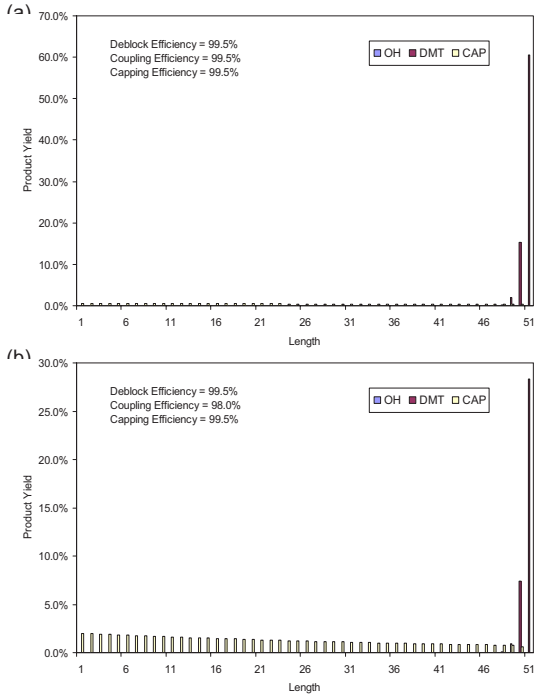

Figure 3.1.2. Effects of coupling efficiency on the synthesis yield of final full-length products after 50 synthesis cycles.

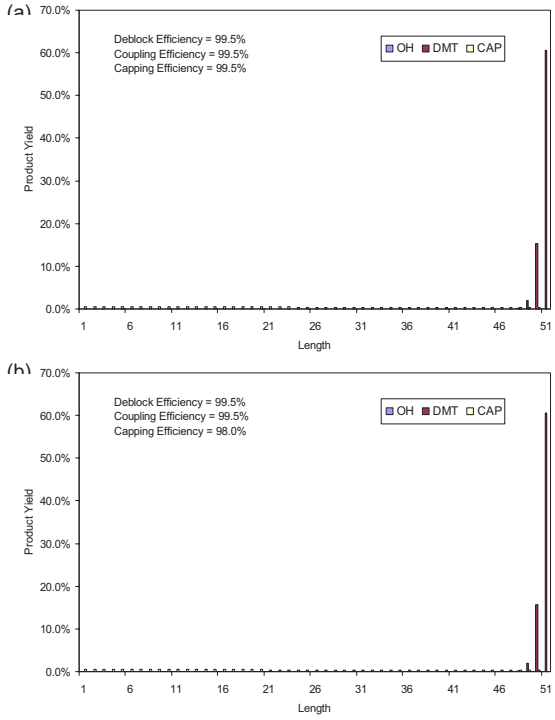

Figure 3.1.3. Effects of capping efficiency on the synthesis yield of final full-length products after 50 synthesis cycles.

3.2. Chemical Confinement during DNA Synthesis Cycle

Based on the digital photolithography technology, photogenerated acid can be produced at desired location by directing light sources to specific reaction cells during DNA synthesis cycles. Although the process is highly controllable, the acid diffusion during repeated synthesis processes could potentially trigger undesirable chemical reactions in the adjacent reaction sites. The cross contamination problem can be further compounded to entire microfluidic system during the wash process that transports chemical mixtures through the entire microfluidic device. Therefore, limiting chemical confinement or more specifically, analyte diffusion during deprotection process becomes a vital requirement for the development of microfluidics based biochips. We undertake this challenge by utilizing numerical simulations to assess the efficacy of analyte diffusion confinements on a microfluidic array platform. The study is designed to demonstrate the transient analyte diffusion characteristics of analyte concentration on the 3D model as showed on Fig. 3.2.1.

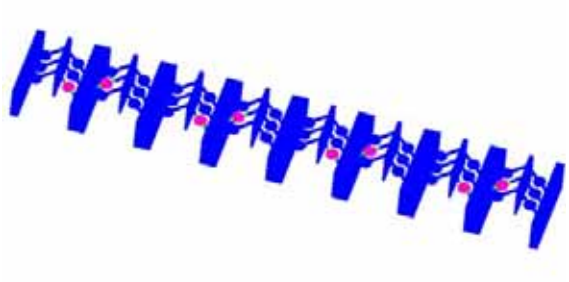

Figure 3.2.1 a 3D computational model.

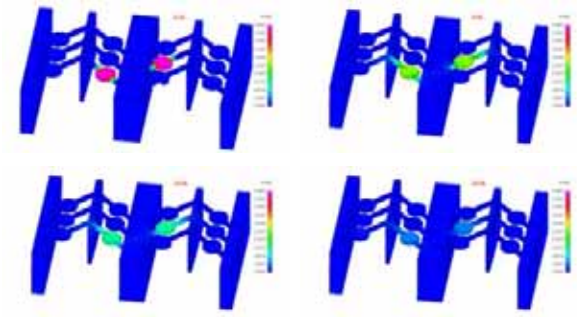

Fig. 3.2.2. Transient analyte concentration distributions at time = 0.1, 5, 10, and 20 seconds. Color red represents the highest value and blue is the lowest value.

The computational model is constructed by the simplified version of channel/reaction-cell

configuration to capture analyte diffusion characteristics without applying a full-scale model which will merely increase computational cost significantly. The model is comprised of total twelve reaction sites and only two source reaction sites with initial analyte concentrations as shown in Figure 3.2.2(a). Figure 3.2.2(a)-(d) demonstrates the transient analyte concentration contours of the current model. Note that the majority of analyte diffuses out of source reaction sites after 20 seconds.

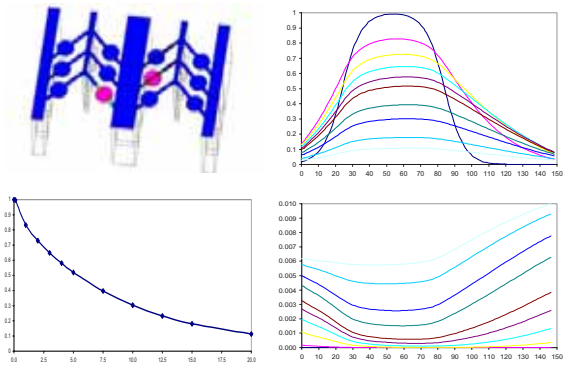

Fig. 3.2.3. (a) Locations of analyte concentration profiles inside two reaction sites. (b) Normalized transient analyte concentration profiles inside the source reaction site at time = 0.1, 1, 2, 3, 4, 5, 7.5, 10, 15, & 20 seconds. (c) Maximum transient analyte concentration values inside the source reaction site. (d) Normalized transient analyte concentration profiles inside the adjacent reaction site at time = 0.1, 1, 2, 3, 4, 5, 7.5, 10, 15, & 20 seconds.

Figure 3.2.3(a) delineates a splice plane of analyte concentration contours of the current computational model. The black straight lines depict the locations of measured analyte concentration profiles inside two reaction cells. Figure 3.2.3(b) shows the normalized transient analyte concentration profiles within the source reaction cell. As we expect, all the concentration profiles exhibit Gaussian like distributions. The peak value of analyte concentration drops to around 63% of initial concentration after 3 seconds which is the approximated time required during the deprotection process of synthesis cycle. The maximum values of normalized analyte concentrations are gradually shifted toward the right side of the source reaction cell due to the larger surface area available on the long conduit side as shown in Figure 3.2.3(c). To assess the efficiency of analyte confinement within the current configuration, the normalized transient analyte concentration profiles inside the adjacent reaction cell are plotted in Figure 3.2.3(d). The maximum analyte concentration entering the adjacent reaction cell is <0.25% of initial concentration after 3 seconds, and it reaches about 1% of initial concentration after 20 seconds. The above simulation results clearly demonstrated that chemical confinement of the current microfluidic biochip throughout entire DNA synthesis cycles can be well-controlled to minimize the severe cross contamination problem caused by the acid diffusion.

CONCLUDSIONS

In this paper, an analytical model has been developed to assess the efficiency of each synthesis step on synthesis yield of final full-length products. Numerical simulations have been employed to further minimize the cross contamination problem of adjacent reaction sites caused by acid diffusion during the deprotection step of each synthesis cycle. For the future works, we intend to incorporate depurination and double coupling effects into DNA synthesis model and continue to utilize detailed numerical simulations to improve the performance of the current microfluidic biochip for multiplex chemical reactions.

ACKNOWLEDGMENT

This research was supported in part by DARPA Micro-Electronics and Bioprocesses (MEB) grant BAA-N39998-01-Q-7057.

REFERENCES

[1] Harrison, D. J., Fluri, K., Seiler, K., Fan, Z., Effenhauser, C. S., and Manz, A., *Micromachining a Miniaturized Capillary Electrophoresis-based Chemical Analysis System on a Chip*, Science 261, pp. 895-897 (1993).

[2] Weigl, B. P., and Yager, P., *Microfluidic Diffusion-based Separation and Detection*, Science 283, pp. 346-347 (1999).

[3] Thorsen, T., Maerkl, S. J., and Quake, S. R., *Microfluidic Large-Scale Integration*, Science 298, pp. 580-584 (2002).

[4] Paul, C. H. Li, and Harrison, D. J., *Transport, Manipulation, and Reaction of Biological Cells On-Chip Using Electrokinetic Effects*, Analytical Chemistry, 69, pp.1564-1568 (1997).

[5] Kopp, M. U., de Mello, A. J., and Manz, A., *Chemical Amplification: Continuous-Flow PCR on a Chip*, Science 280, pp. 1046-1048 (1998).

[6] Gao, X., Yu, P., Leproust, E., Sonigo, L., Pellois, J. P., and Zhang, H., *Oligonucleotide Synthesis using Solution Photogenerated Acids,* J. Am. Chem. Soc. 120, pp. 12698-12699 (1998).

[7] Madou, M., *Fundamentals of Microfabrication*, CRC Press, New York (1997).